PHYSICAL REVIEW E **77**, 020703(R) (2008)

Force between colloidal particles in a nematic liquid crystal studied by optical tweezers

Kenji Takahashi,* Masatoshi Ichikawa, and Yasuyuki Kimura†
Department of Physics, School of Sciences, Kyushu University, 6-10-1 Hakozaki, Higashi-ku, Fukuoka, 812-8581, Japan
(Received 18 June 2007; published 25 February 2008)

We measure the dependence of the interparticle force F on the distance R between two colloidal particles with hyperbolic hedgehog defects in a nematic liquid crystal using optical tweezers. The particle-defect pair can be regarded as an elastic "dipole" in the electrostatic analogy. In a parallel configuration, where the dipole vectors are parallel with each other, F is attractive and proportional to R^{-4}. However, F becomes repulsive at small R due to the existence of a defect between the particles. In an antiparallel configuration, where the particles directly face each other, F is repulsive over the whole range of R and proportional to $R^{-3.6}$. In another antiparallel configuration, where two hyperbolic hedgehog defects directly face each other, F is proportional to $R^{-3.6}$ and F at small R turns out to be attractive upon tilting the dipoles. Furthermore, we yield the force between particles connected by a stringlike defect called a bubblegum defect.

DOI: 10.1103/PhysRevE.77.020703 PACS number(s): 61.30.Jf, 61.30.Gd, 82.70.Dd

A nematic liquid crystal (nematic LC) is an anisotropic fluid, and its molecular long axis points in one direction on average. This direction is represented by a director. In a nematic LC, a singular point where rotational symmetry is broken is frequently observed. This is known as a topological defect. Since these defects cost a large amount of the elastic energy of the LC, they tend to annihilate each other in a uniform LC [1]. Topological defects also emerge due to the existence of colloidal particles in a nematic LC. This is due to the deformation of the local alignment of the LC by the anchoring force at the particle's surface. In this case, the particle itself becomes a topological defect and an additional defect emerges near or around the particle to minimize the elastic deformation of the whole LC. The particle and the accompanying defect strongly couple and move together. Depending on the strength and direction of the anchoring and the size of the particle, three typical types of colloidal particle-defect pair have been reported: "dipole," "Saturn ring," and "surface ring" [2–9]. A specific interparticle force F acts between the particle-defect pairs depending on the configuration. The force is mediated by the elastic deformation of the nematic host [2,8], and is anisotropic and long range compared with the equivalent force in isotropic fluids. In particular, in the case of strong homeotropic surface anchoring, the particle itself becomes a radial hedgehog defect and an additional hyperbolic hedgehog defect appears near the particle at the same time [2,5,8]. This particle-defect pair is called a "dipole" because of its shape and analogous behavior to an electric dipole. The force between such particles has been discussed theoretically in terms of the electrostatic analogy [2,7,8], and the theoretical prediction has been examined experimentally [9,10].

In this paper, we measure the specific interparticle force for three types of configuration, as shown in Fig. 1: a parallel configuration [Fig. 1(a)], an antiparallel configuration (p-p type) [Fig. 1(b)], and another antiparallel configuration (h-h type) [Fig. 1(c)]. In the parallel configuration, two dipoles align in a head-tail arrangement. In the p-p-type antiparallel configuration, two particles face each other with no defects between them. In the h-h-type antiparallel configuration, hyperbolic hedgehog defects face each other.

We used dual-beam optical tweezers to align two particles along the far-field director and to measure the interparticle force F. The optical tweezers have the following advantages: (i) We can measure a force as small as several pN, (ii) we can control the interparticle distance R, and (iii) we can realize situations that are out of equilibrium, as shown in Figs. 1(b) and 1(c).

We dispersed polystyrene latex particles with radii $a = 2.55 \pm 0.1$ μm (Magsphere Inc.) in a nematic liquid crystal MJ032358 (Merck Japan). The refractive index of the particles is 1.6, and the extraordinary and ordinary refractive indices n_e and n_o of the LC are, respectively, $n_e = 1.5$ and $n_o = 1.46$. Therefore, we can stably trap the particles in any direction. The particles were coated with octadecyldimethyl (3-trimethoxysilylpropyl) ammonium chloride (DMAOP) to promote homeotropic anchoring at their surfaces. The particles (<1 wt %) are simply mixed with the LC in the nematic phase, and we stirred the mixture back and forth with a micropipette to achieve good dispersion. After that, the mixture was introduced into a glass cell. The cell surfaces were spin coated with polyimide and rubbed unidirectionally to attain the homogeneous alignment of the LC. The thickness

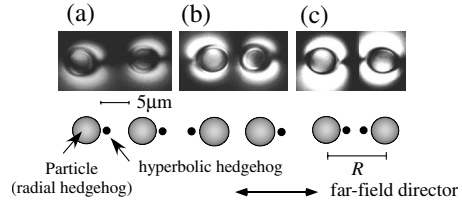

FIG. 1. Various configurations of two elastic dipoles: (a) parallel configuration, (b) antiparallel configuration (p-p type), and (c) antiparallel configuration (h-h type). The upper three photographs were taken under a cross Nicoles polarizing microscope. The lower schematic illustrations correspond to the upper photographs. Each particle-defect pair aligns along the far-field director (horizontal direction in the figure).

*ken8scp@mbox.nc.kyushu-u.ac.jp
†kim8scp@mbox.nc.kyushu-u.ac.jp

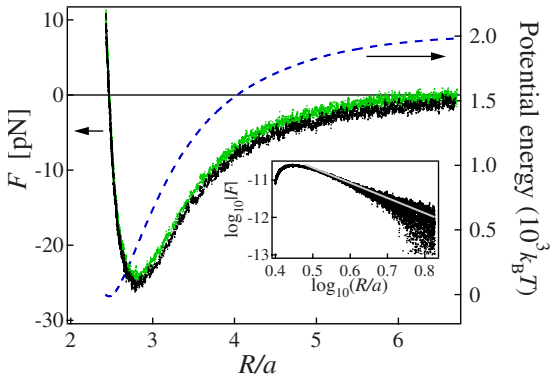

FIG. 2. (Color online) Dependence of the interparticle force F and the potential energy between two particles on the normalized interparticle distance R/a in the parallel configuration. There is slight hysteresis in the force curve. Upper dots (online green) represent F obtained by the approaching process and lower black dots show F obtained by the withdrawing process. The dashed line shows the interaction potential energy. On the left-hand axis, the negative values represent an attractive force and positive values represent a repulsive force. The inset shows the logarithmic plot of F. The slope of the line of best fit, drawn as a solid line, is −4.06.

of the LC sample was fixed using 10-μm spacer films. We used a $Nd:YVO_4$ laser (Spectra Physics, wavelength: 1064 nm) for optical tweezers. The beam is introduced into an inverted fluorescence microscope (TE2000U, Nikon) and focused using a 100× oil immersion objective lens (N.A. =1.3). One of the laser spots was fixed to measure the displacement of the trapped particle in order to calculate F [11,12]. The position of the other laser spot was controlled using two Galvano mirrors (Model 6450, Cambridge Technology Inc.) driven by a two-channel function generator (NF1946). We varied R along the direction of the far-field director as slowly as 100 nm/s to yield F as a function of R. To measure the force, we measured the optical trapping potential from the positional distribution of a particle beforehand. Using the measured potential profile, we obtained the force F from the displacement of the particle from the bottom of the trapping potential of the fixed laser. The shortcomings of this optical method have been pointed out for the application to an LC matrix. It has been reported that the LC alignment is disturbed due to local heating and dielectric interaction at the focal point where the strong light is irradiated [13]. However, by using as weak laser power as possible, we minimized these unfavorable effects. We also subtracted the optically induced force from the obtained bare force by measuring the force between a particle trapped by the fixed laser and the other beam without a particle. The reliability of our method compared with other methods is discussed in detail elsewhere [14].

First, we measured F in the parallel configuration. Figure 2 shows the dependence of F on the center-to-center distance R. At longer distances, F is attractive and obeys $F \propto R^{-4.06}$, as shown in the inset of Fig. 2. From the measurement of five sets of parallel dipoles, the exponent was obtained as -4.01 ± 0.14. On the other hand, at shorter distances, the magnitude of the attractive force decreases with decreasing R, and finally F becomes repulsive. Although we decreased the scanning speed of the laser spot (50 nm/s), the obtained result was unchanged. We calculated the interaction potential energy by integrating F as a function of R, which is plotted in Fig. 2 as a dashed line. The magnitude of the potential was found to be as large as $(2.0 \times 10^3) k_B T$ (k_B, Boltzmann constant: T, absolute temperature).

The dependence at long-to-middle distances is in good agreement with theoretical [2,8], numerical [15,16], and experimental [10,9] results, including those based on the electrostatic analogy. In the case of colloids with the same size a, on the basis of the electrostatic analogy [2,8], the force profile is

$$F = 4\pi K(-6\alpha^2 a^4 R^{-4} + 120\beta^2 a^6 R^{-6}), \tag{1}$$

where α and β are, respectively, parameters concerning the dipole moment and the quadrupole moment, and K is the average elastic constant (the measured value is $K=9.43$ pN). We fitted the experimentally obtained force profile using Eq. (1), assuming that α and β were free parameters, and obtained $\alpha = 1.88 \pm 0.18$ and $\beta = 0.52 \pm 0.12$. These values are in reasonably good agreement with the theoretically predicted values of $\alpha=2.04$ and $\beta=0.72$. On the other hand, the electrostatic analogy cannot be used to explain the force profile, particularly for the repulsive component at a short distance. Although the quadrupolar term in the predicted theory [2,8] can contribute as repulsion and increases at a short distance, its contribution to the total force is expected to be much smaller than the dipolar term [2,8]. The characteristic features of the obtained force curve, such as $F \propto R^{-4.01}$ and the deviation at the short distance, are well explained by recent numerical studies [15,16]. We found that the value of R at rest ($F=0$) is $R/a \simeq 2.47$ from Fig. 2. This is in good agreement with numerical results ($R/a \simeq 2.46$ [15] and $R/a \simeq 2.42$ [16]) and the result of an experiment using magnetic tweezers ($R/a \simeq 2.38 \pm 0.1$ [6]). When two particles approach this distance, the defect between the particles costs a large amount of energy. This is a possible origin of the repulsive component.

In addition to the parallel configuration, we measured F in the particle-facing antiparallel (p-p type) configuration. In this case, we found that F is repulsive over the whole range and is approximately proportional to $R^{-3.6}$, as shown in Fig. 3. From the measurement of five sets, the exponent was obtained as -3.62 ± 0.10.

Although the experimental result $F \propto R^{-3.62 \pm 0.10}$ cannot be explained by the simple electrostatic analogy in which $F \propto R^{-4}$, recent numerical studies [15,16] have reported smaller exponents $F \propto R^{-3.0}$ and $F \propto R^{-3.6}$ at long-to-middle distances. In these studies, the smaller exponents than those for the parallel configuration are due to the strong bare repulsion between two radial hedgehog defects. Although the results of the two numerical studies predict different exponents, the latter [16] is in good agreement with our experimental result. We also found that the data are more scattered than those for a parallel configuration over the whole range. The data scattering at large R in both configurations is due to heat swinging and the measurement accuracy. On the other hand, the data scattering at small R in Fig. 3 is due to the fact

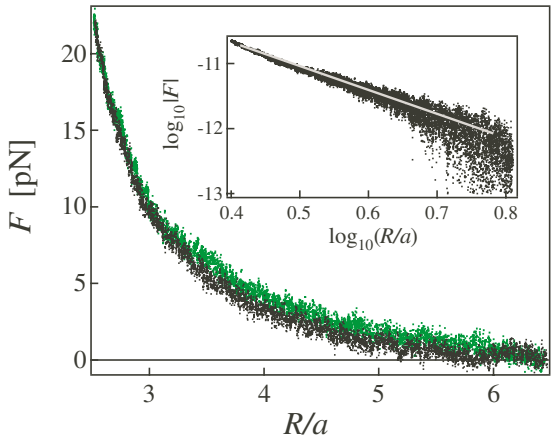

FIG. 3. (Color online) Dependence of the interparticle force F on the normalized distance R/a in the p-p-type antiparallel configuration. Upper dots (online green) represent F obtained by the approaching process and lower black dots by the withdrawing process. On the left-hand axis, positive values represent a repulsive force. The inset shows the logarithmic plot of F. The force is proportional to $R^{-3.68}$, drawn as a solid line.

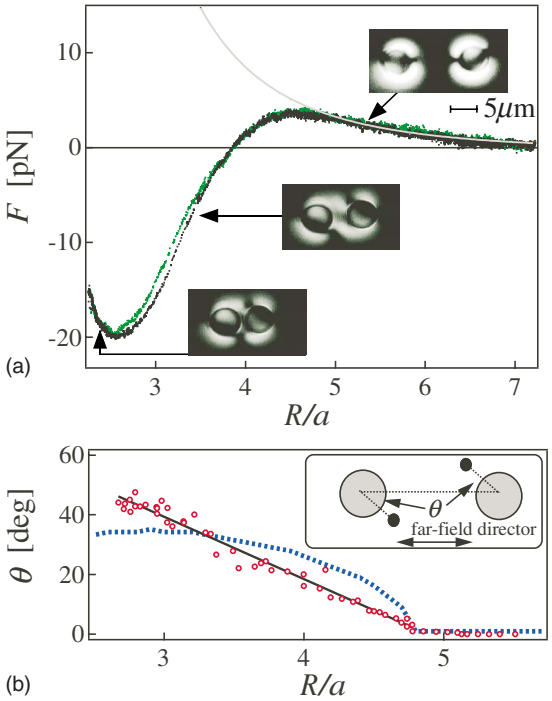

FIG. 4. (Color online) Dependence of the interparticle force F (a) and the angle θ between the elastic dipole and the far-field director (b) on the normalized interparticle distance R/a in the h-h-type antiparallel configuration. The inset photographs were taken under a cross Nicoles polarizing microscope. In (a), upper dots (online green) represent F obtained by the approaching process and lower black dots by the withdrawing process. The solid gray curve shows the curve of best fit, which is proportional to $R^{-3.6}$. Positive values of F represent a repulsive force. In (b), open circles represent experimental data and the black line shows the line of best fit. The dashed line shows the numerical result calculated using the simple electrostatic model.

that this configuration is rather unstable both horizontally and vertically. Nevertheless, we would not be able to observe the change in configuration from antiparallel to parallel even if the optical tweezers did not limit the rotational freedom of each dipole pair. This indicates that there is a high barrier in the pathway of the configuration change from antiparallel to parallel.

We also measured F in the h-h-type antiparallel configuration [Fig. 1(c)] as shown in Fig. 4(a). At long distances, F is repulsive, similar to the p-p case. We can fit the data at larger R with the curve $F \propto R^{-3.60}$, shown as a solid line in Fig. 4(a). At the region where the angle θ between the elastic dipole and the far-field director is nonzero, the force profile diverges from the solid line of $F \propto R^{-3.60}$. As the particles approach each other, the force becomes weaker and finally becomes attractive with increasing θ [Fig. 4(b)]. The angle θ is found to be 0 at large R and has a linear relationship with R. Furthermore, the attractive force has a maximum value at $R \simeq 2.55a$ and the repulsive component emerges at small R. At much shorter distances, we were unable to measure F because the particles move away from the focal plane or the sandwiched defects are transformed into an anomalous defect, as discussed later. In the range of our experiment, there is no significant difference in the profile of F and the defect shape for both approaching and withdrawing processes.

In the attractive range in the h-h-type configuration, the attraction between one particle and the defect belonging to the other particle becomes stronger than the repulsion between the defects. At small R, the repulsion between radial hedgehog defects (particles) may contribute to the reduction of the attractive force. We now attempt to explain the dependence of θ on R using a simple model based on the electrostatic analogy. We consider a particle-defect pair as a dipole composed of the two opposite signs at both ends. The charges corresponding to the particles are fixed, and we calculate the angle θ at which the torque around the fixed charge becomes zero. The torque balance equation is

$$(4d^2 + R^2 - 4dR\cos\theta)^{-3/2} - (d^2 + R^2 - 2dR\cos\theta)^{-3/2} = \frac{E}{Rq}, \tag{2}$$

where d is the length of the dipole (assumed to be $1.24a$), q is the topological charge, and E is the imaginary electric field corresponding to the director field of the LC far from the particles. Using this simple model, we can roughly reproduce the dependence shown as a dashed line in Fig. 4(b); $\theta=0$ at large R and θ increases with decreasing R. However, we cannot obtain the linear dependence of θ on R using this model.

Finally, we have succeeded in producing an exotic defect, which is probably the same type as the "bubblegum defect" [10]. The defect is generated when the h-h-type pairs are forced much closer than the distance shown in Fig. 4. Once this structure has formed, we can stretch it similar to chewing gum by separating the particles. The force F is found to be attractive over the whole range of R, as shown in Fig. 5. In particular, at small R, the attractive force increases slightly

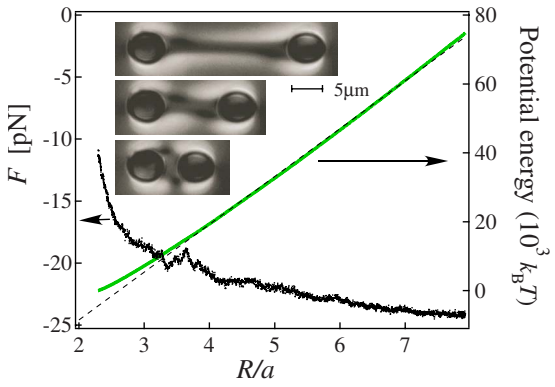

FIG. 5. (Color online) Dependence of the interparticle force F and the potential energy between two particles on the reduced interparticle distance R/a in the bubblegum configuration. The photographs were taken under a cross Nicoles polarizing microscope. The black dots show F and the continuous curve shows interparticle potential. The black dashed line shows the line of best fit to the potential curve at large R. On the left-hand axis, negative values represent an attractive force.

with increasing R. In Fig. 5, we also find that the potential calculated from the dependence of F on R is nearly proportional to R at large R. These characteristics are roughly consistent with previous experimental results [10]. However, there are small and large deviations from the experimental results at larger and shorter distances, respectively. In the preceding experiment [10], F was calculated from the frictional force by assuming constant viscosity regardless of the length of the bubblegum defect. Moreover, the contribution of the hydrodynamic interaction was ignored. These are probable reasons for the above mentioned deviations. On the other hand, a recent numerical study produced a similar result [17], in which the force and potential profiles were in agreement with our result. The origin of the bubblegum defect has not been clarified, but we found, for the first time, that dipolar-type defects can be transformed into bubblegum defects.

In this Rapid Communication, we have reported the interparticle force between dipolar particle-defect pairs in three typical configurations in a nematic LC. In the parallel configuration, the interparticle force is attractive and approximately proportional to R^{-4} at long distances, but the force turns out to be repulsive at short distances. This repulsive component is due to the deformation of the hedgehog defect between the particles. This anisotropic interparticle force, composed of a long-range attractive force and a short-range repulsive force, makes the two particles align along the far-field director without contact [18,19]. In the antiparallel configurations, the results depend on whether or not hyperbolic hedgehog defects exist between the particles. When there is no defect between the particles, the force is repulsive at all distances and is proportional to $R^{-3.6}$. When there are two defects between the particles, the dependence of the force on R is the same as the case for no defect at long distances. However, at short distances, the force is attractive. This is due to the change in direction of the dipole vectors depending on R. Furthermore, we produced a bubble gum defect from dipolar-type defects and identified its interparticle force.

The authors thank Dr. A. Sawada at Merck Japan, Ltd., for providing the liquid crystal sample. They also thank Dr. J. Fukuda (AIST) for valuable discussions. This work was financially supported by a Grant-in-Aid for Scientific Research from the JSPS and on Priority Area "Soft Matter Physics" from MEXT, Japan. M.I. was financially supported by the Sumitomo Foundation and the Sasakawa Scientific Research Grant from the Japan Science Society.

[1] M. Kleman and O. D. Lavrentovich, *Soft Matter Physics: An Introduction* (Springer-Verlag, New York, 2003).
[2] T. C. Lubensky, D. Pettey, N. Currier, and H. Stark, Phys. Rev. E **57**, 610 (1998).
[3] I. I. Smalyukh, O. D. Lavrentovich, A. N. Kuzmin, A. V. Kachynski, and P. N. Prasad, Phys. Rev. Lett. **95**, 157801 (2005).
[4] I. Muševič, M. Škarabot, U. Tkalec, M. Ravnik, and S. Žumer, Science **313**, 954 (2006).
[5] P. Poulin and D. A. Weitz, Phys. Rev. E **57**, 626 (1998).
[6] C. M. Noël, G. Bossis, A.-M. Chaze, F. Giulieri, and S. Lacis, Phys. Rev. Lett. **96**, 217801 (2006).
[7] P. M. Chaikin and T. C. Lubensky, *Principles of Condensed Matter Physics* (Cambridge University Press, Cambridge, England, 1995).
[8] H. Stark, Phys. Rep. **351**, 387 (2001).
[9] M. Yada, J. Yamamoto, and H. Yokoyama, Phys. Rev. Lett. **92**, 185501 (2004).
[10] P. Poulin, V. Cabuil, and D. A. Weitz, Phys. Rev. Lett. **79**, 4862 (1997).
[11] A. Askin, J. M. Dziedzic, J. E. Bjyourkholm, and S. Chu, Opt. Lett. **11**, 288 (1986).
[12] K. Svoboda and S. M. Block, Annu. Rev. Biophys. Biomol. Struct. **23**, 247 (1994).
[13] I. Muševič, M. Škarabot, D. Babič, N. Osterman, I. Poberaj, V. Nazarenko, and A. Nych, Phys. Rev. Lett. **93**, 187801 (2004).
[14] K. Takahashi, M. Ichikawa, and Y. Kimura, J. Phys.: Condens. Matter **20**, 075106 (2008).
[15] J.-I. Fukuda, H. Stark, M. Yoneya, and H. Yokoyama, Phys. Rev. E **69**, 041706 (2004).
[16] J.-I. Fukuda, H. Stark, M. Yoneya, and H. Yokoyama, Mol. Cryst. Liq. Cryst. **435**, 723 (2005).
[17] J.-I. Fukuda and H. Yokoyama, Phys. Rev. Lett. **94**, 148301 (2005).
[18] J. C. Loudet, P. Barois, and P. Poulin, Nature (London) **407**, 611 (2000).
[19] P. Poulin, H. Stark, T. C. Lubensky, and D. A. Weitz, Science **275**, 1770 (1997).